Pergamon

Int. J. Multiphase Flow Vol. 22, No. 3, pp. 485–498, 1996

S0301-9322(96)00002-X
0301-9322/96 $15.00 + 0.00

SMALL CIRCULAR- AND RECTANGULAR-CHANNEL BOILING WITH TWO REFRIGERANTS

T. N. TRAN[1], M. W. WAMBSGANSS[1] and D. M. FRANCE[2]

[1]Energy Technology Division, Argonne National Laboratory, Argonne, IL 60439, U.S.A.
[2]Department of Mechanical Engineering, University of Illinois at Chicago, 842, W. Taylor St., Rm 2039, Chicago, IL 60607-7022, U.S.A.

(Received 2 August 1995; in revised form 29 December 1995)

Abstract—Boiling heat transfer experiments were performed in a small circular channel ($d = 2.46$) and a small rectangular channel ($d_h = 2.40$ mm) with Refrigerant 12. The channel sizes are representative of flow passages in compact evaporators. An experimental technique minimized test section end effects which can be appreciable relative to the heat transfer in these small channels. Local heat transfer results were obtained over a range of qualities up to 0.94, a mass flux range of 44–832 kg/m^{2}s, and a heat flux range of 3.6–129 kW/m^2. Saturation pressure was nearly constant, averaging 0.82 MPa for most of the testing, with some tests performed at a lower pressure of 0.51 MPa. Local heat transfer coefficients were determined experimentally as a function of quality along the length of the test section. Heat transfer rates were compared with results of previous experiments in which Refrigerant 113 in a 2.92-mm diameter small circular tube was used. The effects of channel geometry and fluid properties on heat transfer, as well as insights relative to heat transfer mechanisms in small channels, are presented. Results are presented for both nucleation- (wall superheat above 2.75°C) and convection-dominant boiling heat transfer regimes and compared with large-channel predictions. The heat transfer data for the two fluids were successfully correlated in the nucleation-dominant region. Copyright ©1996 Elsevier Science Ltd.

Key Words: boiling, compact, evaporator, heat transfer, horizontal, nucleation, rectangular channel, refrigerants

INTRODUCTION

Applications of compact heat exchangers for both single- and two-phase flows have been increasing in recent years. To quantify the high surface area-to-volume ratio characteristic of compact heat exchangers, Shah (1986) defined a compact heat exchanger as an exchanger with a surface area density ratio >700 m^2/m^3. This limit translates into a hydraulic diameter of <6 mm. The higher heat transfer surface area density inherent in compact heat exchangers allows attainment of significantly higher heat flux levels in two-phase flows relative to conventional circular tube exchangers. An additional consideration with compact evaporators is the effect of the geometry and size of the flow passage on the two-phase flow and heat transfer phenomena. For example, in noncircular passages of compact evaporators, geometry may influence the liquid inventory (flow pattern) at a given cross section by surface tension and capillary action. The study of boiling heat transfer in the passages of compact heat exchangers translates into the study of boiling phenomena in channels with various small cross-sectional geometries.

Relatively few studies have been reported in the open engineering literature that are directed toward boiling in small passages as compared to single-phase heat transfer in such passages. The two-phase studies can be grouped as: (1) passages in heat exchangers with offset strip fins (Panitsidis *et al.* 1975; Galezha *et al.* 1976; Yung *et al.* 1980; Chen & Westwater 1984); (2) passages in heat exchangers with perforated fins (Panchal 1984, 1989); (3) multichannel arrangements with offset strip fins (Robertson 1979, 1983; Carey & Mandrusiak 1986; Mandrusiak *et al.* 1988; Mandrusiak & Carey 1989); and (4) multichannel arrangements with perforated fins (Robertson & Wadekar 1988; Wadekar 1992). Single-channel studies of flow boiling of Refrigerant-113 (R-113) in a small-diameter circular tube (≈ 3 mm) have been reported by Lazarek & Black (1982) and Wambsganss *et al.* (1993). Boiling in single, small, rectangular passages have been reported by Tran *et al.* (1993) and Peng & Wang (1993). In particular, Tran *et al.* (1993) reported preliminary results of flow boiling of Refrigerant-12 (R-12) in a 1.70×4.06-mm rectangular channel, whereas Peng

& Wang (1993) studied flow boiling of water in a 0.6 × 0.7 mm-rectangular passage.

It has been shown by various experimenters, e.g. Jung *et al.* (1989) and Khanpara *et al.* (1987), that boiling heat transfer of refrigerants in large-diameter channels is controlled by the convection mechanism at qualities >20–30%. In contrast, conclusions differ among the various researchers as to the boiling heat transfer mechanisms in small channels over the entire quality range. Results from tests on actual heat exchangers (Galezha *et al.* 1976; Chen & Westwater 1984; Panchal 1984) suggested a nucleation-dominant mechanism. Galezha *et al.* (1976) showed heat transfer coefficients to vary with heat flux, and Panchal (1984) showed heat transfer coefficients to be insensitive to flow rate. This nucleation-dominant result was supported by investigations of boiling in small smooth channels (circular and rectangular) (Wambsganss *et al.* 1993; Tran *et al.* 1993; Peng & Wang 1993), all of which concluded that a nucleation mechanism dominated the process. Conversely, investigations with multipassage arrangements (Robertson 1979, 1983; Carey & Mandrusiak 1986; Mandrusiak *et al.* 1988; Mandrusiak & Carey 1989; Robertson & Wadekar 1988; Wadekar 1992) all showed nucleation not to be an important mechanism. Heat transfer coefficients were independent of heat flux, dependent on mass flux, and increased with quality (all features of forced convective boiling). This apparent contradiction in conclusions about boiling heat transfer mechanisms in small channels will be reconciled, in part, by the results of this study.

Passage cross-sectional geometry is important to compact heat exchanger design. Recently, preliminary results were reported from the rectangular channel of this study (Tran *et al.* 1993). The data showed nucleation dominance. At that time, data in an equivalent circular channel with the same refrigerant were not available, and comparisons were made between rectangular-channel heat transfer data and the predictions of the Stephan & Abdelsalam (1980) correlation for a circular tube. (Previously, Wambsganss *et al.* (1993) showed that this correlation could predict, with good accuracy, the data for R-113 boiling in a small-diameter circular tube.) As a result of comparing rectangular-channel data with circular-channel correlation prediction, Tran *et al.* (1993) suggested that heat transfer may be more efficient in the small rectangular channel. Results of the present study will, in fact, show that heat transfer rates are comparable for both channels. The reason for the earlier inference is clear and will be discussed.

In the present study, a complete series of 132 tests was performed in the 1.70 × 4.06-mm rectangular channel, and 137 tests were performed in a 2.46-mm diameter circular channel; all tests used R-12 as the boiling fluid. The circular-tube diameter of 2.46 mm was selected to match the rectangular-channel hydraulic diameter of 2.40 mm, thus allowing a direct evaluation of the effect of channel geometry on heat transfer. In addition, R-12 tests in the circular tube were performed over a range of test conditions that facilitates direct comparison with the rectangular-channel data and direct evaluation of the effect of passage geometry. The lower end of the heat flux range (low wall superheat) was also investigated in this study to identify a convective boiling region and provide information on the associated transition from convection to nucleation boiling. Heat transfer results from the two tube passage geometries were compared as part of this work, and the results from the 2.46 mm circular tube are compared with state-of-the-art in-tube evaporation correlations developed for large tubes.

TEST APPARATUS AND INSTRUMENTATION

The test apparatus used for the circular- and rectangular-channel R-12 tests of this study is shown schematically in figure 1. It consists of a closed-loop system with system pressure controlled by high-pressure nitrogen via a pressure regulator and a bladder-type accumulator. The fluid enters the test section in a subcooled state and is evaporated in the test section to a quality of $\approx 80\%$ or less in most tests, depending on mass flux and heat flux. The two-phase mixture leaving the test section is condensed and subcooled before entering the pump. Flow rate is measured with a constant displacement flow meter. The flow meter was calibrated producing an accuracy of better than 2% of the reading.

The system condenser used water at 15°C as the heat sink. The freezer shown in figure 1 allowed further cooling of the refrigerant and was used for lower-pressure testing.

The two test sections (circular and rectangular) were the same length and were instrumented similarly. Based on results of previous investigations (Wambsganss *et al.* 1993; Tran *et al.* 1993;

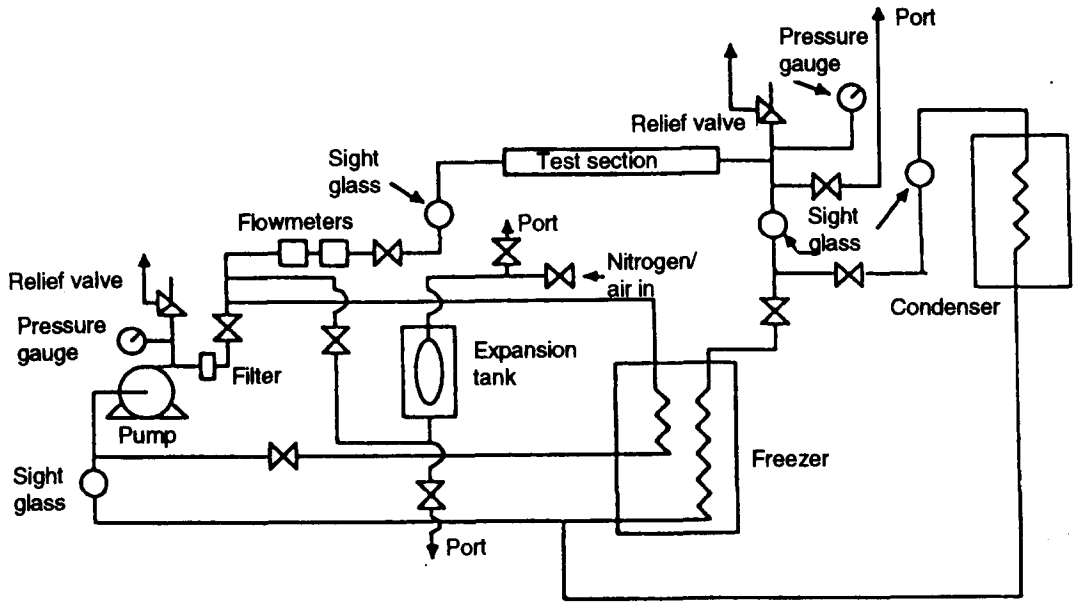

Figure 1. Schematic diagram of test apparatus.

Peng & Wang 1993), nucleation (which in pool boiling is a function of channel material and surface finish) was expected to be the dominant heat transfer mechanism. To eliminate possible effects of tube material on heat transfer, both the 4.06 × 1.70-mm rectangular channel and the 2.46-mm circular tube were fabricated from brass, and to minimize effects of surface condition, both were obtained from the same tubing supplier. The two flow channels each had an overall length of 0.9 m. The channels were resistance heated by passing a DC current through the channel wall. Heat input into the fluid was determined from the electric power input into the channel with an accuracy of 2%, accounting for heat losses to the environment.

Figure 2 is a schematic diagram of the circular-tube flow channel used in this investigation for boiling R-12. Test section features will be detailed by referring to this circular test section; rectangular test section features were similar. Stream temperatures of the bulk fluid in the test section were measured at four axial locations: inlet, outlet, and near two intermediate current clamps. (The test sections were designed to allow variation of heated length using combinations

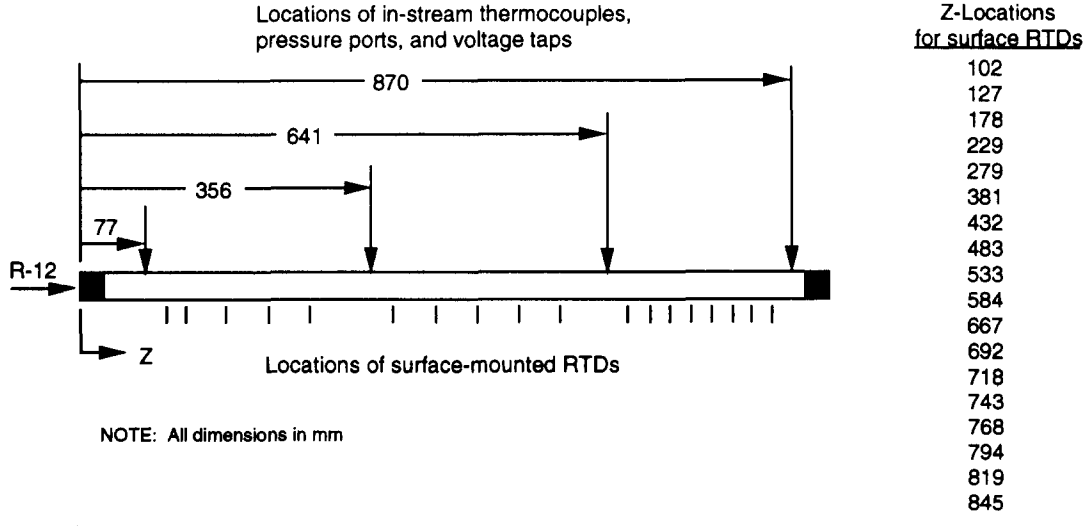

Figure 2. Schematic diagram of circular-tube test section, showing locations of instrumentation (RTD = resistance temperature device).

of four clamps.) These locations are shown in figure 2 at 77, 356, 641, and 870 mm axial locations. Placement of the current clamps and the use of small thermocouple beads to measure stream temperatures between clamps were key features of the test section design. Because of the small channel diameters involved, and the relatively large size of the clamps that were required to carry up to 350 A, heat loss from the clamp areas of the test section could be appreciable. Thus, fluid temperatures were measured between and some distance from the clamps to minimize the effect of this heat loss on the measurements. In addition, the use of four current clamps provided important flexibility in testing parameters. All tests were performed using the exit clamp at 870 mm. Selecting one of the other three clamps for the current path altered the heated length, and thus the heat flux, at a given heating rate.

Pressure ports and voltage taps were provided at each of the four locations where stream temperature measurements were made near the four current clamps on the test section. Both inlet pressure and two-phase pressure drop were measured with calibrated electronic pressure transducers. The inlet pressure was measured with an accuracy of ± 2 kPa, and the test section pressure drop was measured with a differential pressure transducer to an accuracy of ± 1 kPa.

Outside-wall temperatures were measured at various axial locations along the length of the channels by surface-mounted thermocouples for the rectangular channel and surface-mounted resistance temperature devices (RTDs) for the circular tube. (The axial locations of the RTDs are shown in figure 2.) The temperature of the inside surface of the channel was then calculated with the assumption that heat generation in the channel wall was uniform and that the outer surface was well insulated. Liquid tests (isothermal and heat balance) were used to establish uncertainty in temperature measurements of ± 0.2°C. Saturation conditions were used to verify the consistency of both pressure and temperature measurements. More details of the test apparatus are given by Wambsganss *et al.* (1993) and Tran *et al.* (1993).

TEST PROCEDURE AND DATA REDUCTION

Single-phase tests were first performed to check the overall system instrumentation, calibration, and data acquisition equipment and techniques, and to determine heat loss to the environment that was incorporated into the factor η. Single-phase heat transfer coefficients near the test section exit agreed with the Dittus-Boelter correlation within the range of -2 to $+6$%. Isothermal, turbulent experimental friction factors agreed with the Blasius equation within ± 15% over the Re range from 4,000 to 12,000. This good agreement between measured and predicted fully developed heat transfer coefficients and friction factors demonstrated the overall accuracy of the experimental system. Subsequently, a series of flow boiling tests was performed at constant values of mass flux and selected values of heat flux.

The local evaporative heat transfer coefficient was calculated as

$$h(z) = \frac{q''}{T_w(z) - T_{sat}(z)} \quad [1]$$

where the heat flux q'' was calculated as $\eta Q_E / S(L_H - L_{SB})$, ηQ_E is the portion of the electrical power input reaching the boiling fluid, and $S(L_H - L_{SB})$ is the inside surface area of the channel in the boiling region. The quality x at each measurement location z was calculated as

$$x(z) = \frac{S(z - L_{SB})q''}{AG_{i_{fg}}}. \quad [2]$$

In [1], the wall temperatures were measured directly, whereas the saturation temperatures were obtained indirectly from a two-phase pressure drop and exit saturation temperature measurement following a procedure outlined by Tran *et al.* (1993). In this procedure, the saturation temperature was measured at the 870 mm-axial location shown in figure 2 by a very small thermocouple bead located in the fluid stream. By measuring the pressure drop from the start of heating to this exit location, it was possible to determine the saturation temperature at this upstream location in the subcooled region. The length of the subcooled region was determined from a heat balance, and the single-phase pressure drop was calculated. Subtracting the single-phase pressure drop from the pressure at the start of heating gave the saturation pressure (and temperature) at the start of boiling.

Table 1. Test parameter ranges for all tests

Fluid	No. of tests	Channel geometry and size (mm)	P_R	G (kg/m² s)	q'' (kW/m²)	B_o	ΔT_{sat} (°C)
R-12	137	circular $d = 2.46$	0.12 & 0.20	63–832	3.6–59.5	0.00020–0.0017	1.2–6.6
R-113	27	circular $d = 2.92$	0.045	50–400	8.8–90.8	0.00075–0.0023	7.2–18.2
R-12	132	rectangular 1.70×4.06 $d_h = 2.40$	0.20	44–505	5.6–129	0.00028–0.0016	1.8–8.2

The saturation temperature was taken as linear between this point at the start of boiling and the measured saturation temperature at the test section exit. The change in saturation temperature was small (1–2°C) in most tests, and in some cases, a stream temperature measurement, centered in the two-phase region (at 356 or 641 mm in figure 2), served to verify the accuracy of this procedure.

For each of the steady-state tests corresponding to a specific mass flux and heat flux, local heat transfer coefficients were determined for a range of qualities along the length of the test section. In virtually all cases, the heat transfer coefficients were effectively independent of quality for qualities >20%. Measurements that support this finding will be presented, and, in the test results presented subsequently, average heat transfer coefficients, obtained as the average of the measured local heat transfer coefficients for qualities >20%, will be given. Average wall superheats for given test runs were also calculated and used in the presentation of results. The product of the averaged heat transfer coefficient h and wall superheat ΔT_{sat} is equal to the heat flux q''. Further details of these procedures were given by Wambsganss *et al.* (1993) and Tran *et al.* (1993).

EXPERIMENTAL RESULTS

Including data reported by Tran *et al.* (1993), 132 tests for the rectangular channel with R-12 are reported here. A total of 137 new tests for the circular tube are reported with R-12, and these R-12 data are compared with previous circular-tube data with R-113 (Wambsganss *et al.* 1993). The parameter ranges covered by these tests are given in tables 1 and 2.

The heat transfer tests were performed so as to isolate the effects of heat flux, mass flux, and quality. In particular, tests were performed for selected values of mass flux with various heat flux levels, as well as for selected values of heat flux with various mass flux levels.

Uncertainties in heat transfer coefficient were calculated based on the method of sequential perturbations (Moffat 1988). For heat fluxes greater than 12 kW/m² (typically, wall superheats greater than 3°C), uncertainties in heat transfer coefficient were in the range of 6–10%. For heat fluxes less than 12 kW/m² (typically, wall superheats less than 3°C), uncertainties in heat transfer coefficient ranged from 10 to 18%.

Circular channel, R-12 boiling fluid

Results from tests with the 2.46 mm-diameter circular tube and R-12 as the boiling fluid are given in figures 3–5 for wall superheats above 2.75°C. In figure 3, measured local heat transfer coefficients are plotted as a function of quality for approximately constant heat flux values of 7.5, 14.4, and 59.4 kW/m², and, for each value of heat flux, several values of mass flux. It can be observed from the figure that the local heat transfer coefficient is effectively independent of quality for qualities

Table 2. Test parameter ranges for tests with $\Delta T_{sat} > 2.75$°C

Fluid	No. of tests	Channel geometry and size (mm)	P_R	G (kg/m² s)	q'' (kW/m²)	B_o	ΔT_{sat} (°C)
R-12	104	circular $d = 2.46$	0.12 & 0.20	63–832	7.5–59.5	0.00020–0.0017	2.8–6.6
R-113	27	circular $d = 2.92$	0.045	50–400	8.8–90.8	0.00075–0.0023	7.2–18.2
R-12	118	rectangular 1.70×4.06 $d_h = 2.40$	0.20	44–505	7.7–129	0.00028–0.0016	2.8–8.2

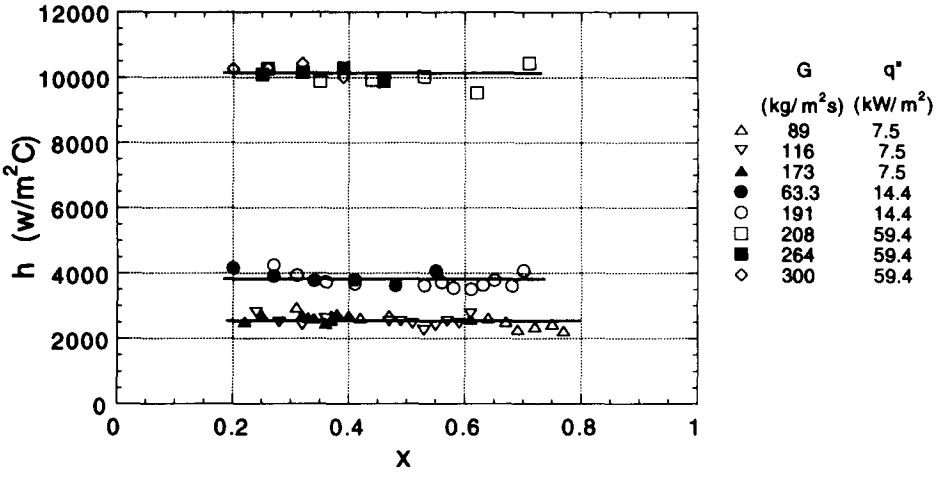

Figure 3. Circular-tube (R-12) local heat transfer coefficients for various combinations of mass flux at three constant values of heat flux and $\Delta T_{sat} > 2.75°C$; $p_{sat} \approx 825$ kPa.

$> \approx 20\%$; this observation supports the use of an average heat transfer coefficient for qualities $> 20\%$. Mass flux independence is also indicated by the data in figure 3.

Average heat transfer coefficients are plotted in figure 4 as a function of mass flux for various constant values of heat flux. The results indicate a strong heat flux dependence and, again, essentially no mass flux dependence.

In figure 5, heat flux is plotted as a function of average wall superheat for all tests in which wall superheat was $> 2.75°C$. Open symbols correspond to the nominal pressure of 0.82 MPa used in this study. The data can be correlated approximately with a straight line when plotted on log–log coordinates, thus indicating a power function relationship between heat flux and wall superheat. Such a functional fit to the data is shown in figure 5, where the correlation coefficient $R = 0.962$.

Although the data in figure 5 show only a heat flux contribution to the heat transfer and no mass flux effect, it is expected that there is a parameter regime where the two phenomena contribute to the heat transfer in small channels, as they do in larger channels. To confirm this point, tests were performed in the circular channel at wall superheats $< 2.75°C$. The results are shown in figure 6 where the lower wall superheats moved the system into a regime where mass flux effects became important. In the figure, two distinct curves can be identified (each having a slope of ≈ 1 on log–log coordinates) that correspond to each of the two values of mass flux tested. It is observed in figure 6 that the division between nucleation- and convection-dominant regions occurs at a wall superheat

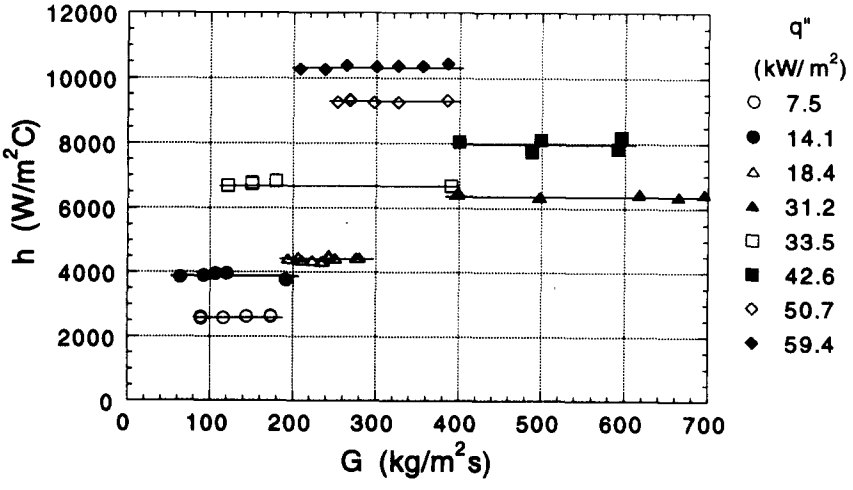

Figure 4. Circular-tube (R-12) average heat transfer coefficients as a function of mass flux for select values of approximately constant heat flux and $\Delta T_{sat} > 2.75°C$; $p_{sat} \approx 825$ kPa.

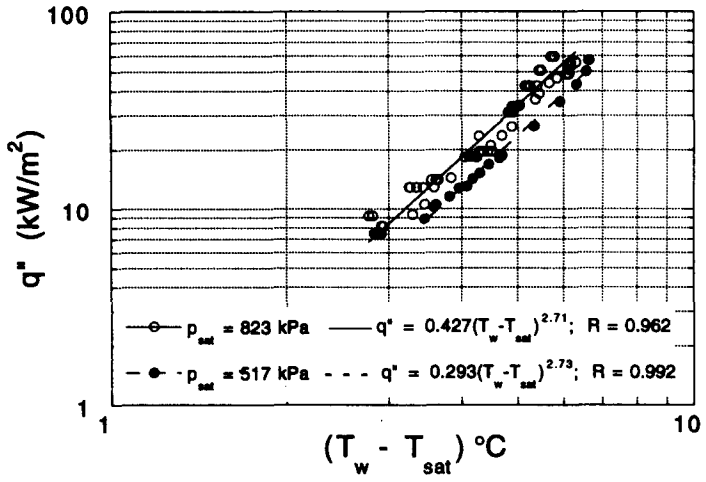

Figure 5. Circular-tube (R-12) heat flux dependence on wall superheat and pressure ($\Delta T_{sat} > 2.75°C$).

of $\approx 2.75°C$. This wall superheat transition marks a major difference between these data and large-tube results as presented in the Discussion section of this paper.

An additional test series was performed with the circular tube at a lower value of saturation pressure. Figure 5 shows the effect of saturation pressure for the data with wall superheat $> 2.75°C$. The results show that the heat transfer rate is sensitive to saturation pressure, and is proportional to it.

Rectangular tube, R-12 boiling fluid

Results from tests with the 4.06 × 1.70-mm rectangular channel are presented in figures 7–9 for wall superheats $> 2.75°C$. These figures correspond to figures 3–5, respectively, for the circular tube with the same fluid. Again, the local heat transfer coefficient was only weakly dependent on quality (see figure 7), allowing for computation of an average heat transfer coefficient. The results presented in figure 8, for average heat transfer coefficient as a function of mass flux for various values of heat flux, show that, for the range of heat fluxes tested, the heat transfer coefficient is effectively independent of mass flux; mass flux independence is also shown by the two sets of data in figure 7.

In figure 9, data from the rectangular-channel tests are plotted in terms of heat flux and average wall superheat. As for the circular tube, the data can be correlated approximately with a straight line on log–log coordinates, indicating a power function relationship between heat flux and wall superheat for $\Delta T_{sat} > 2.75°C$ (as shown in the figure). In figure 9, data obtained at very low values

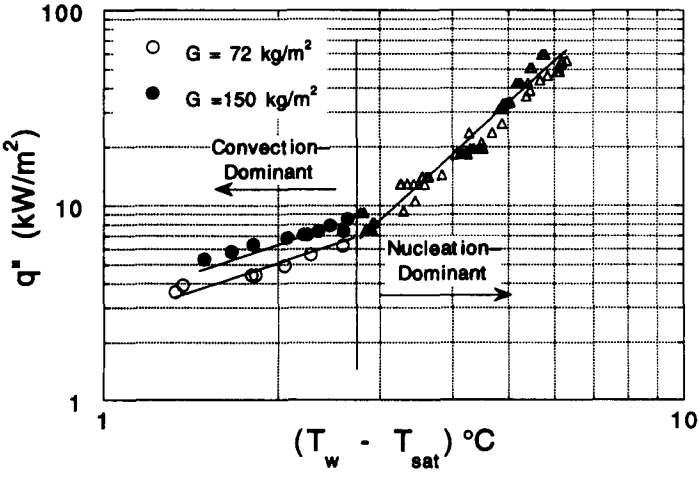

Figure 6. Circular tube (R-12) showing convection-dominant heat transfer at low wall superheat; Δ = all values of mass flux tested; $p_{sat} \approx 825$ kPa.

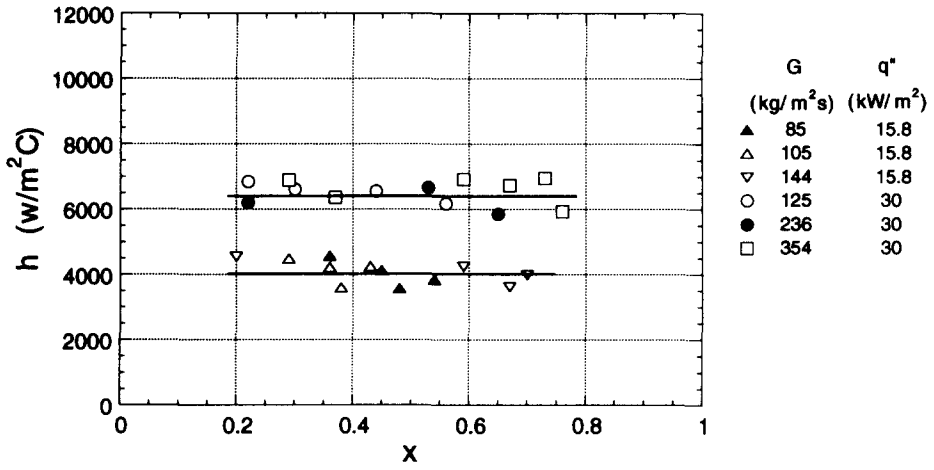

Figure 7. Rectangular-channel (R-12) local heat transfer coefficients for various combinations of mass flux at two constant values of heat flux and $\Delta T_{sat} > 2.75°C$; $p_{sat} \approx 825$ kPa.

of heat flux for two different values of mass flux (80 and 144 kg/m^{2}s) extend the data base to lower values of wall superheat. At the lower values of heat flux, two distinct curves, each with a slope of ≈ 1 on log–log coordinates and corresponding to each of the two values of mass flux tested, can be identified. These mass-flux-dependent results are similar to those shown in figure 6 for the circular tube at low wall superheat $< 2.75°C$.

DISCUSSION

The objectives of this investigation were to (1) further improve our understanding of boiling heat transfer mechanisms in small channels typical of compact heat exchangers, (2) evaluate the effect of flow channel geometry on heat transfer enhancement, (3) predict the boiling heat transfer rates in small channels for the tested refrigerants, and (4) compare small-channel heat transfer behavior with that of large tubes. Each of these subjects is discussed next.

Heat transfer mechanisms

Bulk boiling heat transfer upstream of critical heat flux is governed by the two fundamental mechanisms of forced convection and nucleation. In forced-convection boiling, the heat transfer coefficient is independent of heat flux and dependent on mass flux and quality; heat transfer increases with increasing mass flux and quality. On the other hand, in nucleation-dominant boiling,

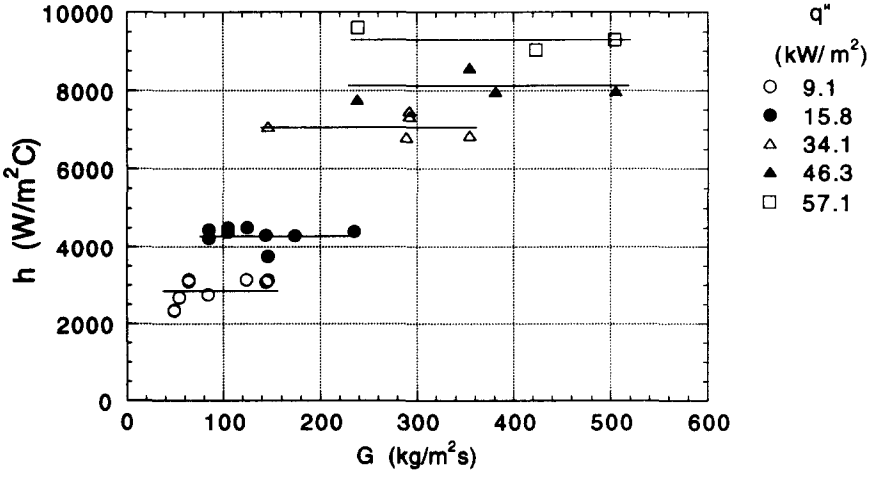

Figure 8. Rectangular-channel (R-12) average heat transfer coefficient as a function of mass flux for select values of approximately constant heat flux and $\Delta T_{sat} > 2.75°C$; $p_{sat} \approx 825$ kPa.

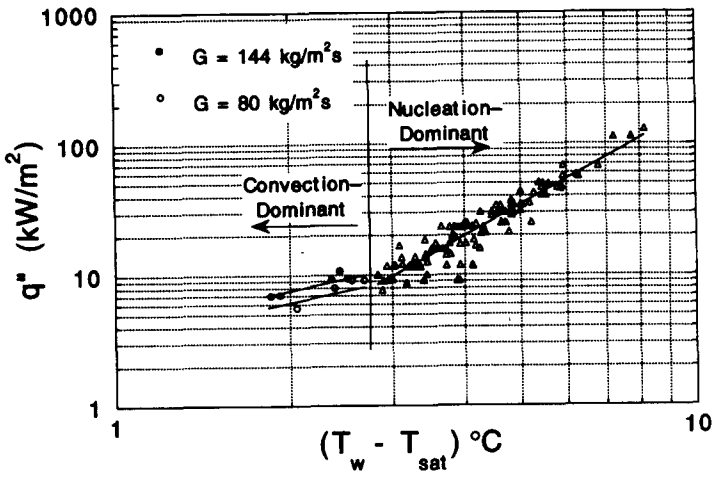

Figure 9. Rectangular-channel (R-12) nucleation- and convection-dominant heat transfer; Δ = all values of mass flux tested; $p_{sat} \approx 825$ kPa.

heat transfer is independent of mass flux and quality, dependent on heat flux, and sensitive to saturation pressure level. Within these parameters, the results shown in figures 3, 4, 7 and 8 lead one to conclude that over a broad range of heat flux, nucleation is the dominant heat transfer mechanism for flow boiling in the small passages considered in this study. This result agrees with previous investigations (Lazarek & Black 1982; Wambsganss *et al.* 1993; Tran *et al.* 1993; Peng & Wang 1993) of flow boiling in small channels. The results of figure 5 show that saturation pressure has a measurable effect on heat transfer, decreasing the heat transfer coefficient as pressure decreases. Because this sensitivity and trend are expected of nucleation-dominant heat transfer, they serve to support the conclusion that a nucleation mechanism dominates.

Although the nucleation mechanism appears to dominate boiling heat transfer in the small channels tested over a broad range of heat flux values, it was expected that, at sufficiently low values of heat flux (very low wall superheat), forced convection will dominate. This was indeed shown to be the case, as illustrated in figures 6 and 9. At wall superheats <2.75°C, the boiling curve is a function of mass flux and the slope of the curve is ≈ 1, implying that the heat transfer coefficient is independent of heat flux. This result is seen in both the circular and rectangular channels.

The transition from convection- to nucleation-dominant boiling is well defined and relatively abrupt for the small-channel data of figures 6 and 9. This abrupt behavior was clearly evident when

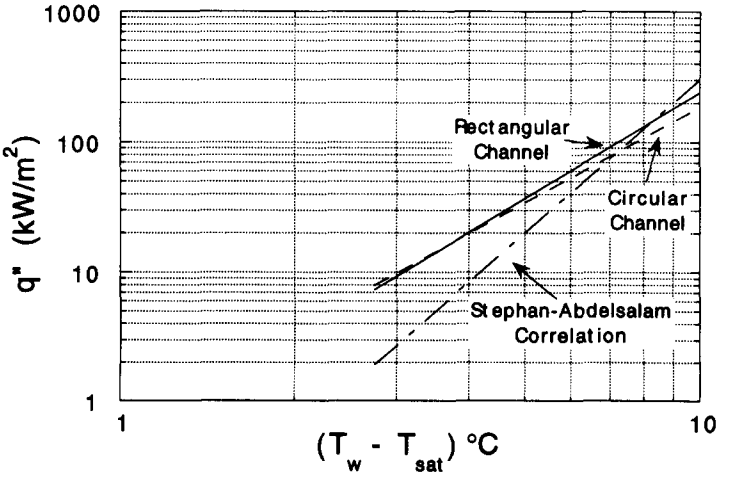

Figure 10. Heat transfer behavior of small rectangular and circular channels and pool boiling prediction of Stephan & Abdelsalam (1980) at $\Delta T_{sat} > 2.75$°C; $p_{sat} \approx 825$ kPa.

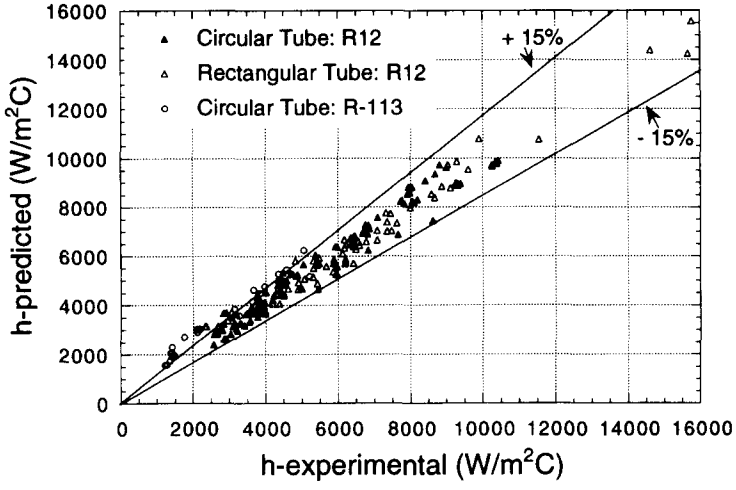

Figure 11. Correlation of nucleation-dominant small-channel data for two fluids and two geometries at $\Delta T_{sat} > 2.75°C$.

data were collected as the system became quasistable at transition and abruptly changed from convection to nucleation dominant. This behavior differs from that found with larger-diameter channels in which relatively broad transition regions occur, typically with contributions from both convection and nucleation boiling being important.

Identification of a convection-dominant region in small-channel boiling heat transfer allows one to reconcile an apparent disagreement between the results of this investigation, and the results of others, e.g. Lazarek & Black (1982), Wambsganss *et al.* (1993), Tran *et al.* (1993), Peng & Wang (1993), who found a nucleation-dominant mechanism; and Robertson (1979, 1983), Robertson & Wadekar (1988), and Wadekar (1992), who concluded from their tests with multichannel arrangements that nucleation is not an important mechanism. The finding of convection dominance by the latter authors was based on data obtained for very low values of wall superheat ($<2.5°C$). The results of this study for very low wall superheats would also lead to this conclusion.

Effect of flow channel geometry

Nucleation-dominant heat transfer data from the circular tube and rectangular channel, both with R-12, were plotted on log–log coordinates as heat flux versus wall superheat in figures 5 and 9, respectively. As shown in those figures, the fact that the data can be reasonably correlated with

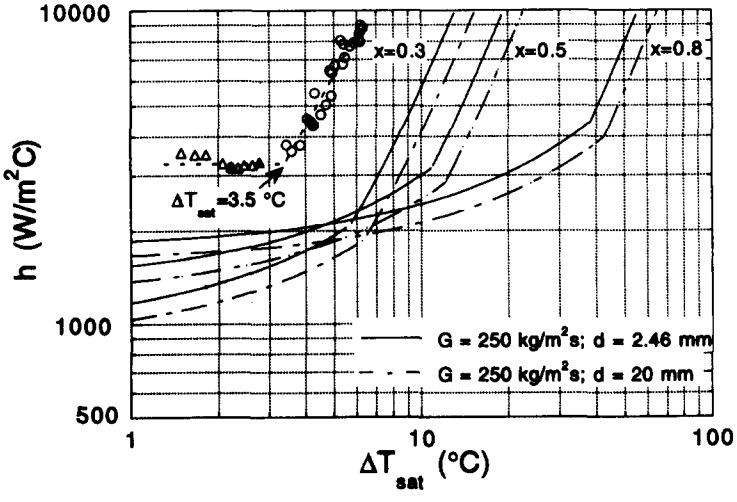

Figure 12. Comparison of the large-tube correlation of Kandlikar (1991) with small circular-tube data (R-12); experimental data: Δ = convection region, $G = 250$ kg/m² s; ○ = nucleation region; $p_{sat} \approx 825$ kPa.

a straight line suggests a power function relationship between heat flux and wall superheat. Therefore, a prediction equation was written in the form

$$q'' = C_1(T_w - T_{sat})^{C_2} \quad [3]$$

where q'' is heat flux in kW/m^2, C_1 and C_2 are constants, and T_w and T_{sat} are tube-wall and fluid-saturation temperatures, respectively, in °C. This is the correlation form for nucleate pool boiling such as that developed by Stephan & Abdelsalam (1980). The constants in [3] were obtained from curve fits to the experimental data for $\Delta T_{sat} > 2.75$°C; the predicted results are plotted in figure 10. The Stephan and Abdelsalam (1980) correlation, which successfully predicted previous small circular-tube data over a range of test conditions with R-113 as the boiling fluid (Wambsganss *et al.* 1993), is also plotted. The results show that there is no significant geometry effect for the two channels tested, each of which has approximately the same hydraulic diameter. At lower values of wall superheat, the Stephan & Abdelsalam correlation significantly underpredicts the data.

As noted in the Introduction, Tran *et al.* (1993) suggested that heat transfer may be somewhat more efficient in a small rectangular channel than in a small circular channel of the same hydraulic diameter. This finding came from a comparison of rectangular-channel R-12 data and state-of-the-art correlations [including the Stephan & Abdelsalam (1980) correlation shown in figure 10] representing R-12 heat transfer in a circular channel. The Stephan & Abdelsalam (1980) correlation gave good predictions of small-channel R-113 data (Wambsganss *et al.* 1993) and was used in the absence of small circular-channel R-12 data. The ΔT_{sat} range of the comparison (Tran *et al.* 1993) was <5°C, which can be seen in figure 10 to be the range where the Stephan & Abdelsalam (1980) correlation is the worst with the R-12 data of this study. It is also clear from figure 10 why the Stephan & Abdelsalam (1980) correlation predicted the R-113 data well when one recognizes that the wall superheat was >6.4°C for all of the R-113 tests. Thus, the inference (Tran *et al.* 1993) that geometry somewhat enhanced heat transfer was a consequence of the underprediction of small circular-tube data by the Stephan & Abdelsalam (1980) correlation at wall superheats <5°C. Comparison of R-12 data from circular channels with that from rectangular channels (see figures 5, 9 and 10), shows that the heat transfer rates are comparable.

Correlation of data

Equation [3] was used to develop a general heat transfer coefficient correlation for the nucleation-dominant regime in the form

$$h = C_3 q''^{C_4} \quad [4]$$

where h is in W/m^{2}C, C_3 and C_4 are constants, and q'' is in kW/m^2. The correlation was based on small-channel boiling heat transfer data with wall superheats >2.75°C for three test sections (circular tube R-12, circular tube R-113, and rectangular channel R-12), and results were employed from the correlation work of Lazarek & Black (1982) which was based on R-113 boiling in a small-diameter (3-mm) tube. This correlation showed some success with the small-channel data of this study; it is based on the Boiling and Reynolds numbers. The exponents of these two dimensionless parameters were such that the mass flux effect was very small, a feature that allowed the correlation to follow the trends, if not the magnitude, of the small-channel nucleation-dominant data. However, recognizing the dominant mechanism to be nucleation rather than convection, the Reynolds number was replaced in this study with the Weber number to eliminate viscous effects in favor of surface tension. Further, accounting for fluid property variations by the liquid to vapor density ratio, the heat transfer data were correlated as follows:

$$h = (8.4 \times 10^{-5})(\mathrm{Bo}^2\mathrm{We}_l)^{0.3}\left(\frac{\rho_l}{\rho_v}\right)^{-0.4}. \quad [5]$$

The units of the average heat transfer coefficient h in [5] are W/m^{2}C.

In figure 11, the predictions of [5] for all of the nucleation-dominant small-tube data of this study are compared with measured experimental values. The circular-tube R-113 data of Wambsganss *et al.* (1993) are also shown in the figure. The comparison is considered very good with most of the data predicted within a 15% random error band and no systematic error observable. The

product of the square of the Boiling number with the Weber number introduces heat flux as the independent variable while mass flux is eliminated. The property effects are correlated through surface tension, latent heat of vaporization, and density ratio, all of which have been used in pool boiling correlation equations.

Large-tube comparison

As a result of the dominance of the nucleation mechanism to high qualities in small-channel boiling, the heat transfer coefficients differ from those that would be expected for large channels with the same mass flux. Comparisons were made with three large-tube correlations that have been developed predominantly for refrigerant flow boiling. The data selected for the comparisons are shown in figure 12. The triangular symbols represent measurements made in the small circular channel of this study, at a mass flux of 250 kg/m^{2}s using R-12; they fall in the convection dominant region. The circular symbols represent measurements in the nucleation dominant boiling region, and here all data are plotted for $G \geqslant 250$ kg/m^2 s because the heat transfer coefficient has been shown to be independent of mass flux in this region.

The first large-tube comparison was made with the Kandlikar (1991) correlation which was developed from a large data base for relatively large-diameter tubes. The results of the large-tube calculations are shown in figure 12, where three values of average quality ($x = 0.3$, 0.5, and 0.8) were chosen to cover the quality range of the data. (A quality of 0.5 is a good choice for the correlation, and the two other values were used to show the sensitivity of the calculations.) Two tube diameters were used with the correlation: one is for a large tube of 20-mm diameter, with $G = 250$ kg/m^2 s, and the other is an extrapolation of the correlation to the tube diameter of the data, $d = 2.46$ mm. The predictions in figure 12 are more sensitive to quality than to tube diameter, but the general trends are all similar, falling well below the data showing significant heat transfer enhancement in the small channel at a given wall superheat.

The Kandlikar (1991) correlation exhibits a clear distinction between nucleation- and convection-dominant boiling regions. The transition between them is seen in figure 12 as the abrupt change in slope of the calculations occurring at $\Delta T_{sat} = 11$ and 12.25°C for the two diameters at a calculational quality of 0.5. The data show this transition at $\Delta T_{sat} \approx 3$°C. With the small tube diameter of 2.46 mm and an average quality of $x = 0.5$, the large-tube correlation predicts convection-dominant heat transfer and low heat transfer coefficients up to wall superheats of 11°C, whereas the small-tube data show the heat transfer coefficient rising sharply in the nucleation-dominant region starting at $\Delta T_{sat} = 3$°C.

Two other correlation equations that were used for comparisons similar to those of figure 12 were the flow boiling correlations of Jung & Radermacher (1991) and Liu & Winterton (1990). Both correlations are based on boiling-refrigerant data in relatively large-diameter tubes. The correlations include both nucleation- and convection-dominant terms, and the change from one to the other is gradual. Comparisons between the predictions of these two correlations and the small-channel data resulted in the prediction of a more gradual transition to nucleation dominance than given in figure 12, but the general results were the same with regard to the underprediction of the data and the overprediction of the wall superheat at transition to nucleation dominance.

CONCLUSIONS

Boiling heat transfer measurements were made with R-12 in a small circular channel ($d = 2.46$ mm) over a substantial range of heat flux, mass flux, and quality. At all but the lowest wall superheats, heat transfer was found to be dependent on heat flux and not on mass flux. This condition had been found previously in a small rectangular channel with R-12 (Tran *et al.* 1993) and in a small circular channel with R-113 (Lazarek & Black 1982; Wambsganss *et al.* 1993). This result implies that the nucleation mechanism dominates over the convection mechanism in small-channel evaporators over the full range of qualities (precritical heat flux qualities of 0.2–0.8) which is contrary to situations in larger channels where the convection mechanism dominates at qualities typically >0.2. This dominant nucleation mechanism contributed to the finding that small-channel heat transfer exhibited an enhancement over predicted large-channel results.

Experiments were conducted at very low wall superheats where, for $\Delta T_{sat} < \approx 2.75°C$, the convection-dominant region was measured. Here, the heat transfer was dependent on mass flux and not heat flux. The transition between regions of nucleation and convection dominance was found to be rather sharp and occurred at significantly smaller values of ΔT_{sat} than predicted for larger diameter tubes. This finding also contributed to the heat transfer enhancement observed for small as compared with larger channels.

Circular- and rectangular-channel data for R-12 and circular-tube data for R-113 in the nucleation-dominant region were correlated by a nondimensional form of the Stephan & Abdelsalam (1980) equation for pool boiling in which the heat transfer coefficient depends on heat flux and not on mass flux. The original Stephan & Abdelsalam (1980) correlation was found to predict small-channel data well at wall superheats $>6°C$.

A comparison was made between the circular- and rectangular-channel data of this study. It was found that very little difference exists between the heat transfer coefficients in a small rectangular channel and a small circular tube with the same hydraulic diameter. The same refrigerant, R-12, was used in both test series.

Acknowledgements—The authors thank Joseph A. Jendrzejczyk for technical contributions during the course of the work, Roger K. Smith for his contributions in fabricating and instrumenting the experiment, and Joyce A. Stephens for preparing the figures and overall manuscript for publication.

This work was supported by the U.S. Department of Energy, Energy Efficiency and Renewable Energy, Office of Industrial Technologies, under Contract W-31-109-Eng-38, and represents a U.S. contribution to the International Energy Agency (IEA) program on Research and Development in Heat Transfer and Heat Exchangers.

NOMENCLATURE

A	Channel cross-sectional flow area (m^2)
B_0	Boiling number ($q''/i_{fg}G$)
d	Channel diameter (m)
d_h	Channel hydraulic diameter (m)
G	Mass flux (kg/m^2s)
$h(z)$	Local heat transfer coefficient (W/m^2C); [1]
h	Average heat transfer coefficient (W/m^2C) from $x = 0.2$ to the test section exit
i_{fg}	Latent heat of evaporation (J/kg)
L_H	Heated length (m)
L_{SB}	Subcooled length (m)
P_R	Reduced pressure
p_{sat}	Saturation pressure (kPa)
q''	Surface heat flux (W/m^2)
Q_E	Heat transfer rate based on electric power input (W)
R	Correlation coefficient
S	Channel circumference (m)
T_{sat}	Saturation temperature (°C)
T_w	Wall temperature (°C)
We_l	Weber number based on liquid ($G^2d/\rho_l\sigma$)
x	Equilibrium mass quality
z	Distance along channel from start of boiling (m)
η	Heat loss factor
ρ_l	Liquid density (kg/m^3)
ρ_v	Vapor density (kg/m^3)
σ	Surface tension (N/m)
ΔT_{sat}	Wall superheat, $T_w - T_{sat}$ (°C)

REFERENCES

Carey, V. P. & Mandrusiak, G. D. 1986 Annular film-flow boiling of liquids in a partially heated, vertical channel with offset strip fins. *Int. J. Heat Mass Transfer* **29**(6), 927–939.

Chen, C. C. & Westwater, J. W. 1984 Application of the local assumption for the design of compact heat exchangers for boiling heat transfer. *J. Heat Transfer* **106**, 204–209.

Galezha, V. B., Usyukin, I. P. and Kan, K. D. 1976 Boiling heat transfer with freons in finned-plate heat exchangers. *Heat Transfer—Soviet Res.* **8**(3), 103–110.

Jung, D. S., McLinden, M., Radermacher, R. & Didion, D. 1989 A study of flow boiling heat transfer with refrigerant mixtures. *Int. J. Heat Mass Transfer* **32,** 1751–1764.

Jung, D. S. & Radermacher, R. 1991 Prediction of heat transfer coefficient of various refrigerants during evaporation. *ASHRAE Trans.* **97**(2), Paper No. 3492.

Kandlikar, S. G. 1991 A model for correlating flow boiling heat transfer in augmented tubes and compact evaporators. *ASME J. Heat Transfer* **113,** 966–972.

Khanpara, J. C., Bergles, A. E. & Pate, B. 1987 A comparison of in-tube evaporation of refrigerant 113 in electrically heated and fluid heated smooth and inner-fin tubes. In *Advances in Enhanced Heat Transfer*—1987, HTD Vol. 68, pp. 35–45. ASME, New York.

Lazarek, G. M. & Black, S. H. 1982 Evaporative heat transfer, pressure drop and critical heat flux in a small vertical tube with R-113. *Int. J. Heat Mass Transfer* **25**(7), 945–960.

Liu, Z. & Winterton, R. H. S. 1990 Wet wall flow boiling correlation with explicit nucleate term. In *Multiphase Transport and Particulate Phenomena* **1,** (Edited by T. Nejat Veziroglu), pp. 419–432. Hemisphere Publishing Corp., New York.

Mandrusiak, G. D., Carey, V. P. & Xu, X. 1988 An experimental study of convective boiling in a partially heated horizontal channel with offset strip fins. *ASME J. Heat Transfer* **110,** 229–236.

Mandrusiak, G. D. & Carey, V. P. 1989 Convective boiling in vertical channels with different offset strip fin geometries. *ASME J. Heat Transfer* **111**(1), 156–165.

Moffat, R. J. 1988 Describing the uncertainties in experimental results. *Exp. Thermal Fluid Sci.* **1,** 3–17.

Panchal, C. B. 1984 Heat transfer with phase change in plate-fin heat exchangers. In *Heat Transfer—Niagara Falls 1984* (Edited by N. M. Farukhi), AIChE Symposium Series, Vol. 80, pp. 90–97.

Panchal, C. B. 1989 Analysis of flow boiling of ammonia and R-114 in a matrix heat exchanger. *Heat Transfer—Philadelphia, 1989* (Edited by S. B. Yilmaz), AIChE Symposium Series, Vol. 85, pp. 293–300.

Panitsidis, H., Gresham, R. D. & Westwater, J. W. 1975 Boiling of liquids in a compact plate-fin heat exchanger. *Int. J. Heat Mass Transfer* **18,** 37–42.

Peng, X. F. & Wang, B.-X. 1993 Forced convection and flow boiling heat transfer for liquid flowing through microchannels. *Int. J. Heat Mass Transfer* **36**(14), 3421–3427.

Robertson, J. M. 1979 Boiling heat transfer with liquid nitrogen in brazed-aluminum plate-fin heat exchangers. In *Heat Transfer—San Diego 1979*, AIChE Symposium Series, Vol. 75, pp. 151–164.

Robertson, J. M. 1983 The boiling characteristics of perforated plate-fin channels with liquid nitrogen in upflow. In *Heat Exchangers for Two-Phase Applications*, HTD Vol. 27 (Edited by J. B. Kitto, Jr & J. M. Robertson), pp. 35–40. ASME, New York.

Robertson, J. M. & Wadekar, V. V. 1988 Boiling characteristics of cyclohexane in vertical upflow in perforated plate-fin passages. In *Heat Transfer—Houston 1988*, AIChE Symposium Series, Vol. 84, pp. 120–125.

Shah, R. K. 1986 Classification of heat exchangers. In *Heat Exchangers: Thermal–Hydraulic Fundamentals and Design* (Edited by S. Kakac, A. E. Bergles & F. Mayinger), pp. 9–46. Hemisphere Publishing Corp., Washington, DC.

Stephan, K. & Abdelsalam M. 1980 Heat transfer correlations for natural convection boiling. *Int. J. Heat Mass Transfer* **23,** 73–87.

Tran, T. N., Wambsganss, M. W., France, D. M. & Jendrzejczyk, J. A. 1993 Boiling heat transfer in a small, horizontal, rectangular channel. *Heat Transfer—Atlanta 1993*, AIChE Symposium Series, Vol. 89, pp. 253–261.

Wadekar, V. V. 1992 Flow boiling of heptane in a plate-fin heat exchanger passage. In *Compact Heat Exchangers for Power and Process Industries*, HTD Vol. 201, pp. 1–6. ASME, New York.

Wambsganss, M. W., France, D. M., Jendrzejczyk, J. A. & Tran, T. N. 1993 Boiling heat transfer in a horizontal small-diameter tube. *ASME J. Heat Transfer* **115**(4), 963–972.

Yung, D., Lorenz, J. J. & Panchal, C. B. 1980 Convective vaporization and condensation in serrated-fin channels. In *Heat Transfer in OTEC Systems*, HTD Vol. 12 (Edited by W. L. Owens), pp. 29–37. ASME, New York.